Available online at www.sciencedirect.com

SciVerse ScienceDirect

Journal of the European Ceramic Society 32 (2012) 1759–1767

www.elsevier.com/locate/jeurceramsoc

# Mechanical and tribological properties of polymer-derived Si/C/N sub-millimetre thick miniaturized components fabricated by direct casting

Vadym Bakumov [a], Gurdial Blugan [a], Sigfried Roos [b], Thomas Graule [a], Vahid Fakhfouri [c], Jonas Grossenbacher [c], Maurizio Gullo [c], Thomas Kiefer [c], Jürgen Brugger [c], Magdalena Parlinska [d], Jakob Kuebler [a,*]

[a] *Empa, Swiss Federal Laboratories for Materials Science and Technology, Laboratory for High Performance Ceramics, Ueberlandstrasse 129, CH-8600 Duebendorf, Switzerland*

[b] *Empa, Swiss Federal Laboratories for Materials Science and Technology, Laboratory for Nanoscale Materials Science Ueberlandstrasse 129, CH-8600 Duebendorf, Switzerland*

[c] *EPFL, Microsystems Laboratory, CH-1015 Lausanne, Switzerland*

[d] *Empa, Swiss Federal Laboratories for Materials Science and Technology, Electron Microscopy Center, Ueberlandstrasse 129, CH-8600 Duebendorf, Switzerland*

Received 11 March 2011; received in revised form 5 January 2012; accepted 7 January 2012
Available online 30 January 2012

**Abstract**

The utilization of silicon-based polymers as a source of amorphous non-oxide ceramics obtained upon pyrolytic treatment of them is increasingly gaining attention in research and is currently expanding into the field of commercial products. This work is focused on the near-net shaped fabrication, mechanical and tribological properties of a polymer-derived Si/C/N system.

Small sub-millimetre thick ceramic test discs and bars were fabricated by casting of polysilazane and/or polycarbosilane precursor mixtures into elastomeric polydimethylsiloxane forms, thermal cross-linking and subsequent pyrolysis. Additional carbon was introduced on the molecular level using triphenylvinylsilane as the precursor, its cross-linking with the polymers via hydrosilylation prohibits phase separation of graphite within the amorphous matrix. The characteristic strength of nearly 700 MPa along with stable low friction coefficients in sliding against similar polymer-derived ceramics testifies to their potential in micro electro mechanical system applications.


*Keywords:* A. Shaping; B. Nanocomposites; C. Strength; D. Carbon; E. Wear parts

## 1. Introduction

Polymer-derived ceramics (PDCs) – are a relatively new class of non-oxide structural and functional materials gaining increasing interest from research and industry.[1,2] The soft nature of the starting polymeric materials provides a unique opportunity for fabrication of various shapes (e.g. by liquid moulding), which are converted into rigid ceramic structures upon curing and subsequent pyrolytic treatment at 600–1000 °C. The tailoring of the chemical structure of the starting polymeric precursor at the molecular level and varying pyrolysis conditions enables adjustment of the resulting composition, microstructure and properties. This approach was successfully commercialized for fibres (e.g. Tyranno Fiber®, Nicalon™)[1a,3] and ceramic matrix composites.[4,1b] It is currently extending into the fields of protective[5,1c] and functional[6,7] coatings, porous bodies,[8,9] filaments[10] and is anticipated to gain a niche in fabrication of miniaturized components. Current micro electro mechanical system (MEMS) technology is mostly based on silicon, whose modest mechanical and tribological properties necessitate the identification and development of new alternative materials.[11,12] Fabrication of various PDC fine structures based on variations in lithographic and soft lithographic techniques was reported over the last decade.[1d,13–16] However, in order to pave the way for a broad use of PDC MEMS, the state of their mechanical and application-specific properties, (e.g. tribological) should be validated. Similar to diamond and DLC,[11] PDCs show low wear friction coefficient in mild operating conditions[17,18] and seem to be promising candidates for MEMS. However, the contact pressures in small moving and sliding parts can exceed

* Corresponding author. Tel.: +41 58 765 4223.
*E-mail address:* jakob.kuebler@empa.ch (J. Kuebler).

0955-2219/$ – see front matter © 2012 Elsevier Ltd. All rights reserved.
doi:10.1016/j.jeurceramsoc.2012.01.007

maximal acceptable Hertzian stresses and lead to severe friction and wear conditions, causing failure.

Among the broad spectrum of preceramic polymers, the family of liquid CERASET® polysilazane[19] precursors which lead to silicon carbonitrides has so far attracted highest attention in the PDC research community, being as well the material of choice for most of the works devoted to PDC MEMS. Additionally silicon oxycarbide[20] and glassy carbon[21] MEMS were presented. Remarkably, polycarbosilane[22] which is industrially used for fabrication of the SiC matrix in disc brakes and is thus promising for other frictional applications has not yet come into the focus of MEMS research.

In the few systematic studies on tribology of PDCs it was shown in the CERASET®-derived Si/C/N system that a transition from mild to severe wear regime occurs after reaching a threshold contact pressure.[17,18] The attractive frictional properties in a mild wear regime were attributed to the free carbon. However, the question of optimal composition in the Si/C/N with respect to strength, friction and wear as well as the requirements and limitations imposed by these materials on engineering applications remain open.

Perhaps the main obstacle which precludes comprehensive and exhaustive characterization of intrinsic properties of PDCs is the difficulty in fabrication of monolithic macro-sized test specimens, the latter is due to cracking caused by substantial gas evolution and shrinkage during pyrolysis.[2d] As already mentioned above, PDC components are made by a number of techniques including, photolithography, soft lithography, moulding and casting of liquid polymers and for larger components using a powder route by warm pressing of partially cross linked (sometimes with fillers) and re-crushed preceramic polymeric powder.[2b] The majority of large bulk test specimens (e.g. 3 mm × 4 mm × 50 mm in dimension) containing a PDC matrix were produced using this powder route.[1e,2a,2b] This technique is not suitable for MEMS fabrication and the mechanical results of these studies are affected by the powder route processing steps. The method of pressure casting reported by Shah and Raj[23] and modified by Janakiraman and Aldinger[24] seems to present a breakthrough in the problem to obtain data which is more relevant to liquid route processed MEMS components. Its applicability for MEMS is however yet to be proven. Test specimens using MEMS fabrication routes tend to have much smaller dimensions e.g. for bending strength specimens these might be typically 1 mm × 3 mm × 0.5 mm in dimension.[25]

Here we report on fabrication of polymer-derived ceramic sub-millimetre-thick components by a direct casting method suitable for production of MEMS test specimens in a size range approximately in between those mentioned above and their characterization with respect to strength, fracture toughness and friction behaviour.

## 2. Experimental

### 2.1. Materials

Commercially available liquid preceramic polymers selected for this study were Ceraset® polysilazane 20 (Clariant Charlotte, NC, USA) and allylhydridopolycarbosilane SMP-10 (Starfire® Systems, Malta, NY, USA). Triphenylvinylsilane (TPVS) – the source of additional free carbon was purchased at ABCR GmbH (Karlsruhe, Germany). 1,1′-Azobis(cyclohexanecarbonitrile) was used as radical initiator for thermal cross-linking of polymeric precursors (Sigma–Aldrich, Buchs, Switzerland). Two-component elastomeric polydimethylsiloxane (PDMS) Sylgard®-184 (Dow Corning, Midland, USA) was used for replication of soft moulds from a SU-8 (MicroChem Corp., Newton, USA) photoresist master. All chemicals were used as received without any purification or modification.

### 2.2. Fabrication

The master SU-8 structures with dimensions of 20 mm × 2.1 mm × 0.3 mm (bars) and 20 mm (diameter) × 0.3 mm (discs) on silicon wafers were created by means of lithography. For the fabrication of PDMS moulds, two components of Sylgard®-184 with mass ratio 1:10 as prescribed by the vendor were mixed, degassed under 2–4 mbar vacuum for 15 min and poured onto a silicon wafer bearing the complementary SU-8 master pattern. After manual tilting of the wafer for a uniform distribution of PDMS, the wafer was placed into a drying box and the temperature was increased to 140 °C with a heating rate of 20–40 °C/h and held for 2 h. After cooling the PDMS replica was gently peeled off, cut into circles of 50 mm diameter and glued with the unstructured side onto 7 mm thick PTFE discs, which act as a rigid support for flexible PDMS. For the fabrication of thicker (0.6 mm) PDC specimens the corresponding cavities were ground directly in PTFE discs (depth ∼0.8 mm). The precursors were mixed in the proportions given in Table 1, using for the sake of homogeneity and process acceleration a small ultrasonic horn (5 W) for 30–60 s (liquid is heated up to 60 °C). The mixtures were degassed at 0.3–0.5 mbar for 20–30 min whilst intensively stirring (800–1100 rpm) and thereafter cast using a micropipette into previously lubricated (with silicon grease) PDMS moulds. The usefulness of the degassing procedure is dictated by the fact that both preceramic polymers contain volatile oligomers and slowly expel hydrogen and/or ammonia even during normal storage, causing macroporosity and even bloating of the samples upon heating and evaporation of dissolved volatile species. Caution was paid to the volume injected into the mould cavities in order to minimize the meniscus built on the top. For the fabrication of PDC counter bodies for tribological tests, drops of precursor were placed directly onto PTFE support without PDMS. Due to the high contact angle between polymers and PTFE the drops do not spread and solidify during cross-linking in the form of hemispheres. The latter being pyrolytically converted into ceramics were glued onto an aluminium pin and fixed to a strain gauge in a tribometer (see next paragraph). The filled supported moulds are stacked onto each other and transferred into a hermetically tight Büchi miniclave chamber (Büchi AG, Uster, Switzerland) which is evacuated and flushed with argon twice. Thereafter, Ar pressure of 3 bar is

Table 1
Composition of precursor mixtures.

| Sample | PSZ 20 [wt.%] | SMP-10 [wt.%] | TPVS [wt.%] | R.I. [wt.%] | Pyrolysis | Hv 0.5 [GPa] | Density [g/cm$^3$] |
|---|---|---|---|---|---|---|---|
| A | 49 | 40 | 10 | 1 | 1370 °C, Ar, closed boat | 11.2 ± 0.3 | 2.29 |
| B | 79 | 10 | 10 | 1 | 1370 °C, $N_2$, open boat | 13.5 ± 0.7 | 2.27 |
| C | 99 | 0 | 0 | 1 | 1370 °C, Ar, closed boat | – | – |
| D | 0 | 99 | 0 | 1 | 1370 °C, Ar, closed boat | 12.6 ± 0.3 | – |
| E | 0 | 89 | 10 | 1 | 1370 °C, Ar, closed boat | 13.7 ± 0.5 | – |
| F | 0 | 94 | 5 | 1 | 1370 °C, Ar, closed boat | 14.0 ± 0.3 | – |
| H[a] | 59 | 40 | 0 | 1 | 1370 °C, Ar, closed boat | 9.5 ± 1 | – |
| I | 89 | 0 | 10 | 1 | TGA, 1300 °C open boat | – | – |

[a] 0.6 mm thick samples, casted in PTFE.

applied and the chamber is heated to the target temperature of 165–175 °C over a 4 h period using a silicon oil bath and kept at 175 °C overnight for cross-linking. After cooling, the solidified samples are released mechanically from the moulds, placed into open or closed SiC boats and pyrolyzed in an alumina tube furnace (Carbolite STF 16/610, Carbolite Ltd., Hope Valley, UK) under flowing nitrogen (Alphagas1, purity 99.999%) up to the target temperature. The heating and cooling rates were 0.45 and 3.3 K/min respectively, the annealing time was 2 h.

### 2.3. Characterization

The strength of rectangular specimens was measured on a Zwick-testing machine Z005 (Zwick GmbH, Ulm, Germany) in 3-point-bending mode using an 8 mm span, 0.2 N preloading force and 0.5 mm/min cross-head speed. The data was processed according to two-parameter Weibull statistics using maximum likelihood regression. Fracture toughness was measured according to single edge V-notched beam method[26] on four 0.6-mm bars of material H (Table 1). For this purpose a ∼0.1 mm deep notch was polished in the middle of the bars using a steel razor blade and diamond grinding paste. The bars were loaded in 3-point bending mode (I-mode) similarly to the strength tests described above. Hardness was measured on a Leitz Durimet microhardness tester equipped with a Vickers indenter using a 500 g load. A home-made tribometer comprising of a linear actuator and strain gauge detecting the tangential force was used for friction measurements. The disc specimens were glued onto the stage driven by the actuator, the counter body was loaded with a prescribed weight, fixed to a strain gauge and was brought in contact with the specimen to achieve sliding friction. FT-IR spectra were measured on a Golden Gate ATR. Scanning electron micrographs were acquired on VEGA Tescan (Brno, Czech Republic) using acceleration of 10 kV and secondary electron detector. Raman spectra were taken on Renishaw RM1000 (Renishaw Inc., Gloucestershire, UK) equipped with Leica DMLM optical microscope using excitation wavelength of He/Ne Laser (633 nm). High resolution transmission electron microscopy (HR-TEM) was performed on crushed bulk samples using a 2200FS TEM/STEM (JEOL, Japan) operated at 200 kV.

## 3. Results and discussion

### 3.1. Fabrication PDC specimens by direct casting and pyrolysis

The compositions of samples used for this study (Table 1) are dictated by the aim to reveal the effect of the precursor on the process of fabrication, the microstructure, mechanical and tribological properties of macroscopic PDCs. The fabrication of freestanding test specimens faces several challenges which arise from expelling of volatile species and shrinkage during both stages of cross-linking and pyrolysis. Among the series of Ceraset® products,[19] the Polysilazane 20 (PSZ 20) has a lower difference between densities of liquid and cured solid compared to polyureasilazane. In order to minimize shrinkage during cross-linking and tensions associated with it, we chose the former one. The SMP-10 polycarbosilane has a density of ∼1.0 g/cm$^3$ both in the raw and cured states. The challenge of gas expulsion and bloating can be addressed by keeping the thickness of the polymer layer below 0.7 mm whilst using degassing and a slow uniform heating as described in Section 2. The peculiarity of the presented approach is the absence of hermetically tight pressurized moulds used in[23,24] and thus its suitability for MEMS. Further challenges of cracking and/or deformation arise during the stage of pyrolysis and were described in the literature.[24] Variation of experimental parameters (composition, heating- and gas flow rates, sample geometry and dimensions, holder, etc.) allowed us to ascertain the origin of forces acting on a specimen during pyrolysis leading to a non-uniform shrinkage within the specimen and discern external and internal factors affecting form fidelity. The external factors are those conditions of pyrolysis, which determine the uniformity of heat distribution and its transfer to the sample, i.e. thermal conductivity of the specimen holders, length of the heating zone and gas flow rate. The flow of inert gas which protects specimens from oxidation was in our experiments the main source of temperature perturbations and must be reduced to the minimum level, yet remain high enough to maintain low overpressure inside the tube and prohibit air entrapment into the heating zone.

Internal parameters inherent to the specimen are the stiffness of the green body, presence of curvature and the aspect ratio. Thicker discs were less prone to warpage than the thinner ones. Additionally, we found that the degree of deformation

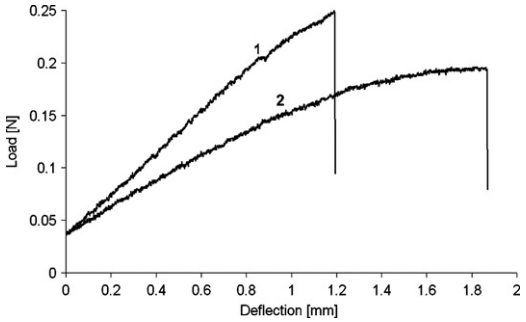


Fig. 1. Load-deflection curves of 3-point-bending tests of green preceramic bars (20 mm × 2.2 mm × 0.25 mm) (1) based on 100% of Ceraset® PSZ 20 (mixture C), (2) with addition of 60 wt.% of SMP-10. Increase of polycarbosilane fraction results in less stiff specimens.

correlated with the content of SMP-10 precursor and thus with flexibility of the green bodies (Fig. 1). Furthermore, discs and bars with larger diameters and length respectively were more deformed, than those with smaller linear dimensions. The direction of warpage during pyrolysis was pre-determined by the curvature of the surface, which stems from the meniscus built on the top of the liquid prior to solidification. Positive curvature (derived from convex meniscus) as well as the negative one (concave meniscus) increased in magnitude during pyrolysis affecting also the initially flat counter side. Flat samples (negligible curvature) being exposed to considerable temperature gradient, e.g. created due to a high flow rate of inert gas experienced extensive cracking (Fig. 2). Small cracks on the edge of flat specimens grew, if the latter were exposed to non-optimized pyrolysis conditions. These deformations occurred at temperatures below 500 °C, cracks appeared in the temperature range 540–570 °C. These observations could be explained as follows. The temperature gradient which is created along the sample due to external factors of limited thermal conductivity and/or due to cooling by a stream of inert gas causes different shrinkage and stresses within it. Larger samples were exposed to larger differences in temperature on the opposite ends and offered leverage for warpage-causing tensions, whereas high stiffness (E-Modulus) and thickness of the samples (internal factors) resist deformation. The presence of positive or negative curvature of the surface (with Laplace pressure directed outwards or inwards respectively) triggers the direction of forces determining thus the convex or concave form of the sample and relieves the tensions.

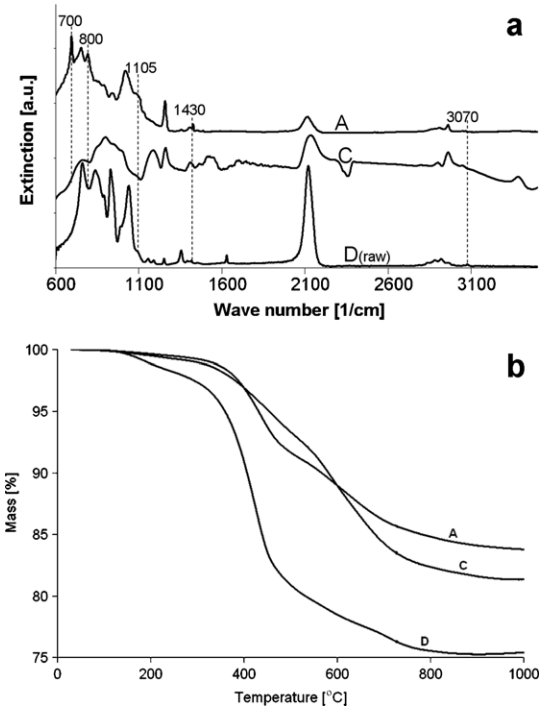


Fig. 3. (a) IR-spectra of specimens given in Table 1 demonstrate bonding and conservation of TPVS in the cured polymeric precursor matrix, the maxima of absorption bands of aromatic fragments are marked; (b) thermogravimetric curves of cross-linked specimens with compositions given in Table 1.

### 3.2. Phase composition

Carbon species, homogeneously distributed within an amorphous Si/C/N matrix are regarded as the lubrication component[17,18] in PDCs. On the another hand, poor mechanical and wear properties of graphite should restrict it's content for structural applications and necessitate the possibility of controlled introduction of non-crystalline carbon into the starting materials. This can be achieved using triphenylvinylsilane (TPVS) as the carbon source which is soluble in preceramic polymers and bonds to them during cross-linking via hydrosilylation (Fig. 3a). The absorption bands of aromatic fragments, which were not present in the green bodies C and D were attributed as follows: 700 $cm^{-1}$: C–H bend out of plane; 800 $cm^{-1}$: Si–$C_{Ph}$ stretch; 1105 $cm^{-1}$: C–H bending in plane; 1430 $cm^{-1}$: C=C stretch; 3070 $cm^{-1}$: C–H stretch. The rest

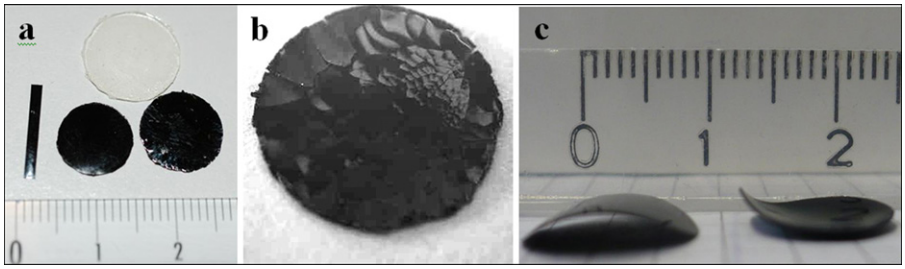


Fig. 2. (a) Casted and cross-linked transparent polysilazane disc and resulting ceramics: intact bar and disc (left), cracked disc (right); (b) surface of disc from (a) pyrolized under high flow rate of nitrogen reveals severe chipping; (c) convex (left) and concave (right) discs pyrolized under moderate flow rate (∼5 $cm^3$/min) of nitrogen.

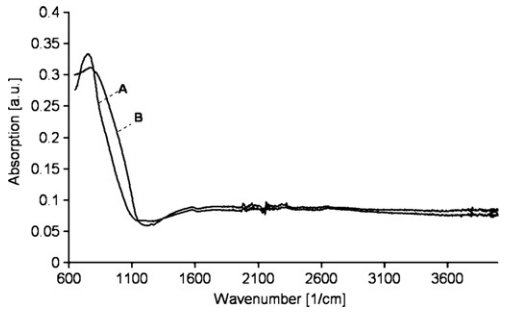


Fig. 4. Absorption spectra of powdered specimens A and B reveal higher amount of Si–N bonds in material B as a shoulder in short-wavelength region of Si–C band.

of spectral features of commercial precursors were described previously in literature.

As a result of the bonding, the conservation of carbon from TPVS is achieved, as indicated by thermal gravimetry (Fig. 3b), which shows same ceramic yield for polysilazane modified with 10% of TPVS and the pure one (mixtures I and C respectively). Indeed, since the major mass loss during pyrolysis is determined by the degree of reticulation then such monofunctional agents as TPVS which does not promote cross-linking cannot also affect the amount of ceramic residue. The substitution of 40% of CERASET® in the mixture I by SMP-10 (mixture A) leads to increase of the ceramic yield by 2% due to the enhanced cross-linking between polysilazane and polycarbosilane chains. The increased ceramic yield of polysilazane–polycarbosilane mixture as compared to pristine constituents was described by Motz previously.[27]

Increased polycarbosilane content leads to a SiC-enriched sample A, the sample B shows detectable amount of Si–N bonds (Fig. 4).

The pyrolysis conditions influence the composition as well and whereas pyrolysis under a stream of nitrogen (specimen B) results in silicon carbonitride ceramics,[19] the treatment under standing atmosphere consisting predominantly of expelled hydrocarbons, leads to carbon enriched SiC (specimen A). These variations along with the polycarbosilane content determine the composition of the Si/C/N and have a strong effect on the tribology.

X-ray diffraction pattern (Fig. 5a) reveals β-silicon carbide nanocrystals and amorphous carbon. The absence of graphite crystalline phases in carbon-enriched material A, treated at temperatures as high as 1370 °C can be attributed to extensive cross-linking within the matrix which creates high interconnectivity of the 3D polymer network in the present system restricting the chain mobility and low diffusion coefficients of amorphous Si/C/N/H hybrid materials (duromers) make crystallization of

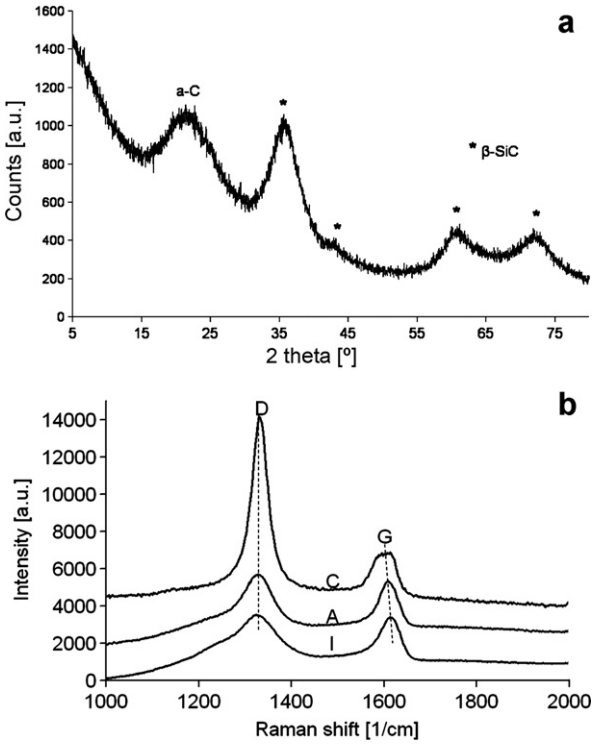


Fig. 5. (a) X-ray diffraction pattern of ceramic A pyrolized at 1370 °C; (b) Raman spectra of PDC samples with only PSZ 20 (C), with TPVS(I), and with TVPS and SMP 10 (A).

graphitic carbon not possible. The Raman spectra of the specimens show peculiar D and G peaks of carbon centered at 1330 and ca 1610 $cm^{-1}$ respectively (Fig. 5b), each was fitted with two Lorentzian curves. The decreasing width of the G-peak and intensity of D-peak in the series of samples C to I (Table 2) reflect continuously increasing degree of ordering of the "free" carbon species within covalent Si/C/N matix.[28] This tendency coinsides with the slightly increasing vibrational energy of the G peak (1603–1614 $cm^{-1}$) and points thus on the preservation and/or condensation of the carbon rings from the carbon source TPVS into layers within pyrolized samples. On the other hand, broadening of the G peak and increase of the relative intensity of the D peak when moving from sample I to additive-free sample C leads to conclusion about the first stage in the "amorphization trajectory"[28] for carbon-enriched samples and existence of carbon species in predominantely $sp^2$-form ordered in nanocrystalline graphite clusters.

High resolution transition electron microscopy (HR-TEM) supports the above conclusions and further clarifies the influence of carbon precursor on the microstructure of the ceramics: sample H without any additional carbon sources consists of a

Table 2
Raman analysis of carbon scattering peaks after fitting with Lorentzians.

| Sample | G-peak position [1/cm] | G-peak HWHM [1/cm] | D-peak position [1/cm] | D-peak HWHM [1/cm] | $I$(D)/$I$(G) [a.u.] |
|---|---|---|---|---|---|
| C | 1603 | 69 | 1331 | 42 | 3.2 |
| A | 1610 | 55 | 1328 | 79 | 1.06 |
| I | 1614 | 56 | 1327 | 106 | 0.96 |

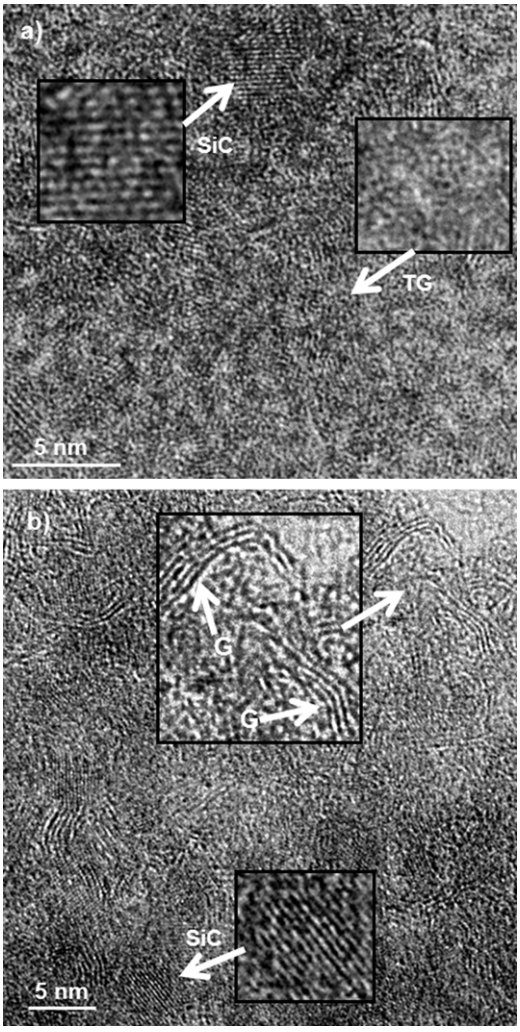


Fig. 6. High resolution transition electron microscopy (HR-TEM) images of (a) sample H without additional carbon showing a structure of β-SiC nanocrystals and turbostratic graphite (TG) and (b) sample A showing a microstructure of β-SiC nanocrystals, turbostratic graphite (TG) and graphitic carbon (G).

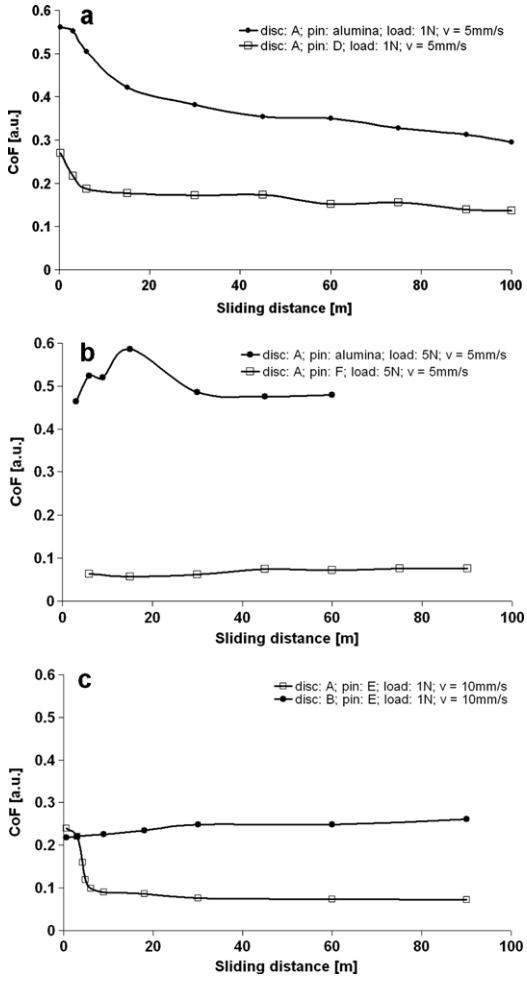


Fig. 8. Evolution of coefficient of friction during continuous sliding: (a) A against alumina counter body as compared to SiC derived from SMP-10 both at 1 N load and 5 mm/s sliding velocity. (b) A against alumina and against SiC with 5% of additional carbon (F) at both at 5 N load and 5 mm/s sliding velocity. (c) Counter body derived from SMP-10 with ca. 10% of additional carbon (mixture E) in sliding against A and B both at 1 N load and 10 mm/s sliding velocity.

microstructure of occasional β-SiC nano crystallites with sizes ranging from 2 to 10 nm in a mixed matrix of amorphous and turbostratic graphite (Fig. 6a).

The HR-TEM indicates also that the addition of carbon via TPVS precursor leads to a number of changes in the microstructure of the sample A (Fig. 6b). Firstly there is an increase in the number of the β-SiC nanocrsytallites, and whilst some turbostratic graphite is still visible, there is now also additional graphitic carbon with clearly visible interlattice planes. Such tiny soft inclusions do not constitute flaws and therefore do not deteriorate strength but significantly improve tribological properties of the materials (see next sections).

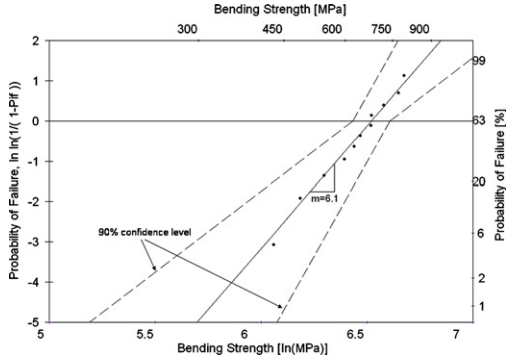


Fig. 7. Weibull plot for 3-point bending tests of rectangular bars (20 mm × 1.5 mm × 0.18 mm) of material A.

### 3.3. Mechanical properties

The difficulties in direct fabrication of monolithic carbon-[29] and silicon-based[2] test samples have restricted characterization of their intrinsic mechanical properties so far. A characteristic strength of 1100 MPa for polished pressure-casted Ceraset®-derived ceramics was reported.[23] However, the microstructure, particularly the porosity of PDCs is highly process-related and any variations in the preparation steps make the mechanical properties difficult to predict. For the samples prepared in the

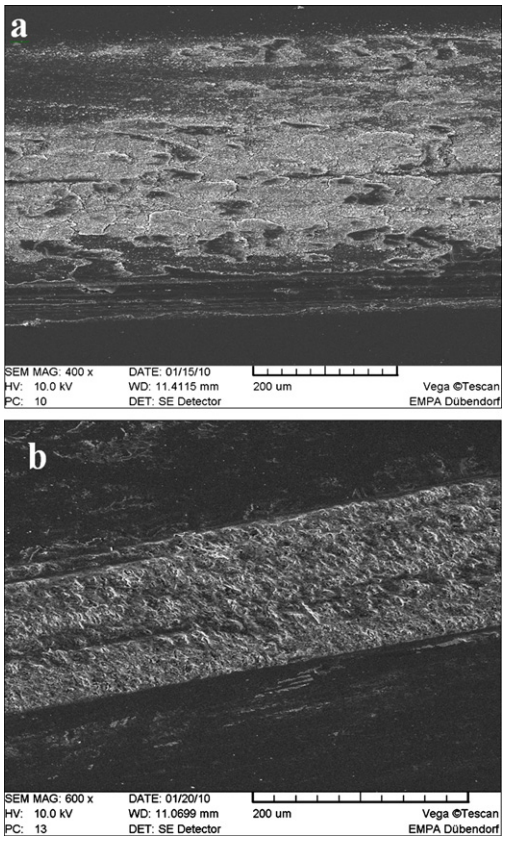


Fig. 9. Wear track of sample A after sliding against alumina (1 N, 14 mm/s, 100 m) directly after testing (a) and after removing of debris in ultrasonic bath (b).

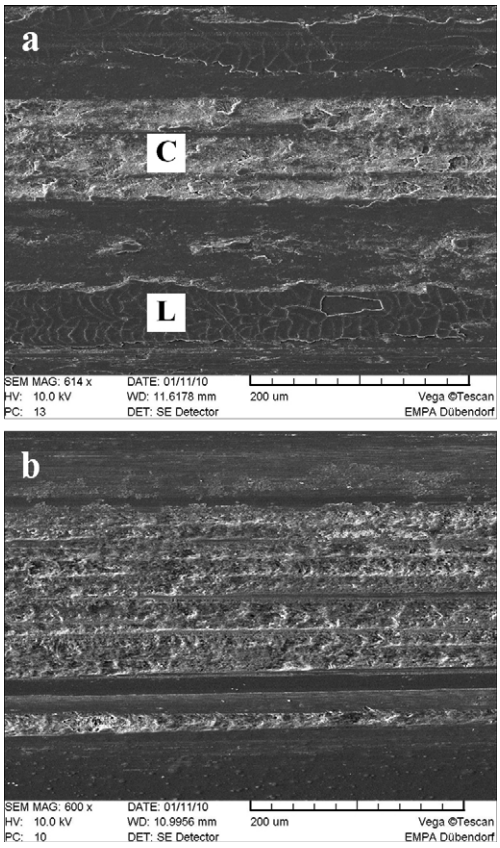


Fig. 10. Comparison of wear tracks on sample B. (a) After sliding against alumina (1 N, 14 mm/s, 100 m); (b) against SiC derived from SMP-10 (1 N, 5 mm/s).

present study the 3-point bending tests (Fig. 7) revealed a characteristic strength of approximately 700 MPa, which slightly exceeds that obtained for unpolished pressure-casted samples prepared by Shah and Raj.[23] In our experiments the variations in content of SMP-10 in the range of 0–50 wt.% and pyrolysis temperature (1130–1370 °C) did not affect the strength significantly and slight variation in the value could be mostly attributed to the statistical nature of the parameter. Indeed, the relatively low Weibull modulus of 6.1 in the present work resembles highly probabilistic behaviour of glass fibres,[30] whereas pressure-casted samples by Shah and Raj[23] revealed higher (polished) or lower (unpolished) flexural strength. For such low toughness materials[31] the surface finish of the specimens is the key factor with respect to strength and the small size of MEMS should make them an appropriate niche for PDCs' application. It was also possible to fabricate 0.6 mm thick bars of composition H for SEVNB, whilst thick samples with other compositions usually suffered from cracking during pyrolysis. The material H reveals toughness of $1.3 \pm 0.2$ MPa $m^{1/2}$. This value roughly corresponds to that evaluated by Janakiraman et al. for a Ceraset®-derived Si/C/N annealed at the same temperature range.[31] To the best of our knowledge it is the first report on fracture toughness of monolithic filler-free Si/C/N PDCs measured by SEVNB mode-I loading technique.

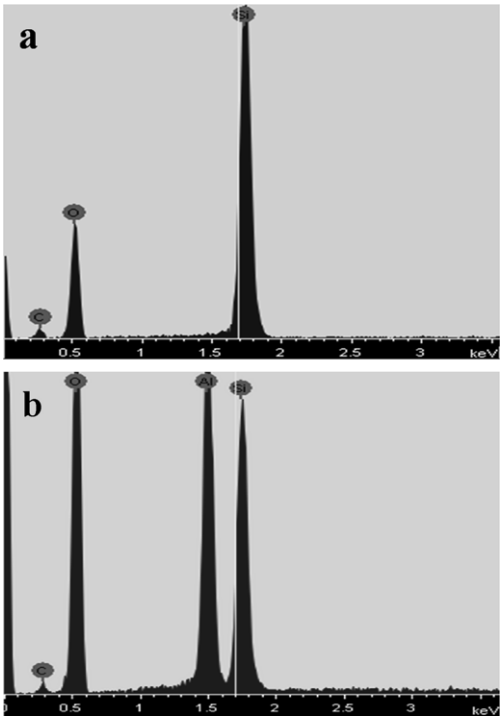


Fig. 11. EDX spectra taken on wear track of sample B: (a) from center ("C" in Fig. 10a); (b) from lateral sediment spurs (L in Fig. 10a).

### 3.4. Tribological properties

The potential of PDCs for tribological applications was recognized nearly a decade ago.[32,33] In systematic studies on polysilazane-based systems the increase of performance with increasing annealing temperature was reported[18] and the material of the counter body, either alumina or steel, was found to be irrelevant to the characteristics of friction.[17] In the present study PDC counter bodies revealed a lower coefficient of friction (CoF) compared to alumina and the difference was more pronounced with increasing load (Fig. 8a and b). This observation can be attributed to the higher carbon content in the contact zone and/or reduced Hertzian contact stress due to a lower Young's-Modulus of amorphous PDCs compared to alumina. Indeed, the content of TPVS-derived carbon in the pin lowers the CoF against material A (Fig. 8a and c). The SiC-enriched sample A perfoms better than B (Fig. 8c), one of the possible explanations is the thermal conductivity of nanocrystalline SiC which results in faster heat dissipation. Remarkable here is the absence of a soft graphite (Fig. 5) despite the presence of additional carbon source (TPVS) indicating efficiency of cross-linking reactions in impeding graphitization. The amorphous carbon is an excellent lubricating constituent, which does not suffer from poor mechanical properties as its graphitic counterpart. The measured hardness (Table 1) supports this conclusion. All the materials tested reveal comparable hardness, which is far below that of 15–26 GPa obtained by Shah and Raj,[23] but slightly exceeds that measured by Janakiraman and Aldinger.[24] The strong impact of pre-pyrolytic processing and other parameters on mechanical properties has been stressed by Janakiraman and Aldinger[24] and we believe that the remarkably lower hardness of material H (Table 1) has to be attributed to the increased thickness of the test specimens (0.6 mm vs. 0.2 mm for the rest of the samples).

SEM observation of the wear tracks reveals a peculiar behaviour of the debris: in contrast to the wear track of material A (Fig. 9), which is covered and probably thus protected by debris, the aluminium-containing debris are shifted to the periphery in the sample B (Figs. 10 and 11). This continuously exposes fresh surface to the friction stresses leading to a greater degree of wear.

## 4. Conclusions

Small PDC objects with one of the dimensions below 1 mm can be fabricated by direct casting, cross-linking and pyrolysis of polysilazanes and polycarbosilanes. Adjustment of the matrix composition and content of additional carbon can be achieved by proper choice of preceramic polymers, directed addition of carbon precursor and pyrolysis conditions. The resulting ceramics reveal considerable strength (~700 MPa) and low coefficient of friction (<0.1) in sliding against PDCs. Decrease of CoF is achieved by increase of carbon and/or SiC content. This combination of properties is highly promising for MEMS applications.

## Acknowledgements

This research was sponsored by the Innovation Promotion Agency CTI of Switzerland, project number CTI 9611.1 PFNM-NM. Authors are grateful to Dr. F.A. Nüesch for access to IR-spectrometer, Dr. P. Hug for Raman spectra and appreciate the technical assistance of H.-J. Schindler and R. Bächtold.

## References

1. Colombo P, Soraru G-D, Riedel R, Kleebe H-J. *Polymer derived ceramics: from nano-structure to applications*. DEStech Publications; 2009, 476 pp. see: (a) Chapter 5.3 by Motz G and Bernard S, p. 341; (b) Chapter 5.8 by Sherwood WJ, p. 402; (c) Chapter 5.4 by Scheffler FA and Torrey JD, p. 363; (d) Chapter 5.9 by Schultz M, p. 417; (e) Chapter 5.1 by Bakumov V and Kroke E, p. 309 and references therein.
2. (a) Reviews on PDCs: Riedel R, Mera G, Hauser R, Klonczynski A. Silicon-based polymer-derived ceramics: synthesis properties and applications. *J Ceram Soc Jpn* 2006;**114**(6):425–44;
(b) Colombo P, Mera G, Riedel R, Soraru G-D. Polymer-derived ceramics: 40 years of research and innovation in advanced ceramics. *J Am Ceram Soc* 2010;**93**(7):1805–37;
(c) Bill J, Aldinger F. Precursor-derived covalent ceramics. *Adv Mater* 1995;**7**(9):775–87;
(d) Greil P. Polymer derived engineering ceramics. *Adv Eng Mater* 2000;**6**(2):339–48.
3. Okamura K, Shimoo T, Suzuya K, Suzuki K. SiC-based ceramic fibers prepared via organic-to-inorganic conversion process – a review. *J Ceram Soc Jpn* 2006;**114**:445–54.
4. Sherwood WJ, Whitmarsh CK, Jacobs JM, Interrante LV. Low cost near-net shape ceramic composites using resin transfer molding and pyrolysis (RTMP). *Ceram Eng Sci Proc* 1996;**17**(4):174–83.
5. Torrey RK. Mechanical properties of polymer-derived ceramic composite coatings on steel. *J Eur Ceram Soc* 2008;**28**:253–7.
6. Cross TJ, Raj R, Prasad SV, Tallant DR. Synthesis and tribological behavior of silicon oxycarbonitride thin films derived from poly(urea)methyl vinyl silazane. *Int J Appl Ceram Technol* 2006;**3**:113–26.
7. Bakumov V, Gueinzius K, Hermann C, Schwarz M, Kroke E. Polysilazane-derived antibacterial silver–ceramic nanocomposites. *J Eur Ceram Soc* 2007;**27**:3287–92.
8. Schmidt H, Koch D, Grathwohl G, Colombo P. Micro-/macroporous ceramics from preceramic precursors. *J Am Ceram Soc* 2001;**84**(10):2055–252.
9. Bakumov V, Schwarz M, Kroke E. Emulsion processing of polymer-derived porous Si/C/(O) ceramic bodies. *J Eur Ceram Soc* 2009;**29**(13):2857–65.
10. Colombo P, Perini K, Bernardo E, Capelletti T, Maccagnan G. Ceramic microtubes from preceramic polymers. *J Am Ceram Soc* 2003;**86**:1025–7.
11. Krauss AR, Auciello O, Gruen DM, Jayatissa A, Sumant A, Tucek J, et al. Ultrananocrystalline diamond thin films for MEMS and moving mechanical assembly devices. *Diamond Relat Mater* 2001;**10**:1952–61.
12. Williams JA, Le HR. Tribology and MEMS. *J Phys D: Appl Phys* 2006;**39**:R201–14.
13. Liew LA, Luo R, Liu Y, Zhang W, An L, Bright VM, et al. Fabrication of multi-layered SiCN ceramic MEMS using photo-polymerization of precursor. In: *Proc. 14th annual international conference on micro electromechanical systems (MEMS2001)*. 2001. p. 86–9.
14. Lee H-J, Yoon T-H, Park J-H, Perumal J, Kim D-P. Characterization and fabrication of polyvinylsilazane glass microfluidic channels via soft lithographic technique. *J Ind Eng Chem* 2008;**14**:45–51.
15. Schulz M, Boerner M, Hausselt J, Heldele R. Polymer derived ceramic microparts from X-ray lithography – cross-linking behavior and process optimization. *J Eur Ceram Soc* 2005;**25**:199–204.
16. Fakhfouri V, Jiguet S, Brugger J. Surface micromachining of polyureasilazane based ceramic-MEMS using SU-8. Micromolds. *Adv Sci Technol* 2006;**45**:1293–8.

17. Klaffke D, Wäsche R, Janakiraman N, Aldinger F. Tribological characterisation of siliconcarbonitride ceramics derived from preceramic polymers. *Wear* 2006;**260**:711–9.
18. Cross T, Raj R, Prasad SV, Buchheit TE, Tallant DR. Mechanical and tribological behavior of polymer-derived ceramics constituted from $SiC_xO_yN_z$. *J Am Ceram Soc* 2006;**89**:3706–14.
19. Information on Ceraset® polysilazanes is available from vendor at http://www.kioncorp.com.
20. Liu X, Li Y-L, Hou F. Fabrication of SiOC ceramic microparts and patterned structures from polysiloxanes via liquid cast and pyrolysis. *J Am Ceram Soc* 2009;**92**(1):49–53.
21. Schueller OJA, Brittain ST, Whitesides GM. Fabrication of glassy carbon microstructures by soft lithography. *Sens Actuators* 1999;**A72**:125–39.
22. Information on polycarbosilane SMP-10 is available from vendor at http://www.starfiresystems.com.
23. Shah SR, Raj R. Mechanical properties of a fully dense polymer derived ceramic made by a novel pressure casting process. *Acta Mater* 2002;**50**:4093–103.
24. Janakiraman N, Aldinger F. Fabrication and characterization of fully dense Si–C–N ceramics from a poly(ureamethylvinyl)silazane precursor. *J Eur Ceram Soc* 2009;**29**(1):163–73.
25. Namazu T, Ishikawa T, Hasegawa Y. Influence of polymer infilitration and pyrolysis process on mechanical strength of polycarbosilane-derived silicon carbide ceramics. *J Mater Sci* 2011;**46**:3046–51.
26. Kübler J. In: Bradt RC, Munz D, Sakai M, Shevchenko VYa, White KW, editors. *Fracture toughness of ceramics using the SEVNB method: a joint VAMAS/ESIS round robin, fracture mechanics of ceramics*, vol. 13. Kluwer Academic/Plenum Publishers; 2002. p. 437–45.
27. Motz G. Synthesis of SiCN-precursors for fibres and matrices. *Adv Sci Technol* 2006;**50**:24–30.
28. Ferrari AC, Robertson J. Resonant Raman spectroscopy of disordered, amorphous, and diamond like carbon. *Phys Rev B* 2001; **64**:075414.
29. Jenkins GM, Kawamura K. *Polymeric carbons – carbon fibre, glass and char*. Cambridge University Press; 1976.
30. Pirhonen E, Moimas L, Brink M. Mechanical properties of bioactive glass 9–93 fibres. *Acta Biomater* 2006:103–7.
31. Janakiraman N, Burghard Z, Aldinger F. Fracture toughness evaluation of precursor-derived Si–C–N ceramics using the crack opening displacement approach. *J Non-Cryst Solids* 2009;**355**: 2102–13.
32. Seitz J, Bill J, Aldinger F, Naerheim Y. Process for producing a Si/C/N ceramic body, US6458315, 2002.
33. Greil P, Dernovsek O, Güther H-M, Wislsperger U. Molded part of ceramic material derived from polymers, process for producing ceramic molded parts and sliding element having a molded part. US6709999, 2004.